Electronic Supplementary Material (ESI) for ChemComm.

Electronic Supplementary Information

In situ monitoring of vapour-induced assembly of pharmaceutical cocrystals using a benchtop powder X-ray diffractometer

Igor Huskić, Jan-Constantin Christopherson, Krunoslav Užarević and Tomislav Friščić

Table of Contents

1. Methods and Materials

Chemicals used in the experiments were used as obtained. Carbamazepine (**cbz**) powder, nicotinamide (**na**), fumaric acid (**fum**), suberic acid (**sub**) and sacharine (**sac**) were obtained from Sigma Aldrich.

Milling of the samples was performed using a MM200 Retsch shaker mill operating at 25 Hz, in polytetrafluoroethylene (PTFE) jars of 14 mL volume and using two stainless steel balls of 8 mm diameter (1.4 g weight). Total mass of the reaction mixture never exceeded 300 mg. Each reaction mixture was milled for 15 s to ensure homogeneity of the sample.

Powder X-ray diffraction (PXRD) data was collected on a Bruker D2 Phaser LYNXEYE^{TM} instrument using nickel-filtered CuK_α (λ = 0.154056 Å) radiation.

Fourier-transform infrared attenuated total reflectance (FTIR-ATR) measurements were performed on a Bruker VERTEX 70 instrument equipped with a PLATINUM diamond crystal ATR unit.

Thermogravimetric and differential scanning calorimetry (TGA and DSC) analysis was performed on a Mettler-Toledo TGA DSC 1 Star system thermobalance and Mettler-Toledo DSC 1 Star system differential calorimeter using alumina crucibles under an stream of air or nitrogen (50 ml min^{-1}) and a heating rate of 5 °C min^{-1} or 10 °C min^{-1}, depending on the experiment. Sample size was between 5 mg and 10 mg. Results were processed with the Mettler STARe 9.01 software.

***In situ* XRPD monitoring** was performed by placing a small amount (30 mg) of the premilled material on the custom-made sample holder made of polymethylmethacrylate (PMMA). 100 µl of liquid were pipetted into the grooves on the holder, while making sure no liquid touches the sample. Vacuum grease was applied to the outer ledges of the holder to ensure airtightness. A small piece of thin low-density polyethylene (LDPE) foil (*Glad Wrap*®) was applied to the top of the holder and gently pressed to seal the edges. The holder was then placed in the XRPD instrument and the collection was commenced immediately. Temperature of the sample chamber varied in the range 30 ± 2 °C, as established by monitoring with a thermocouple sensor.

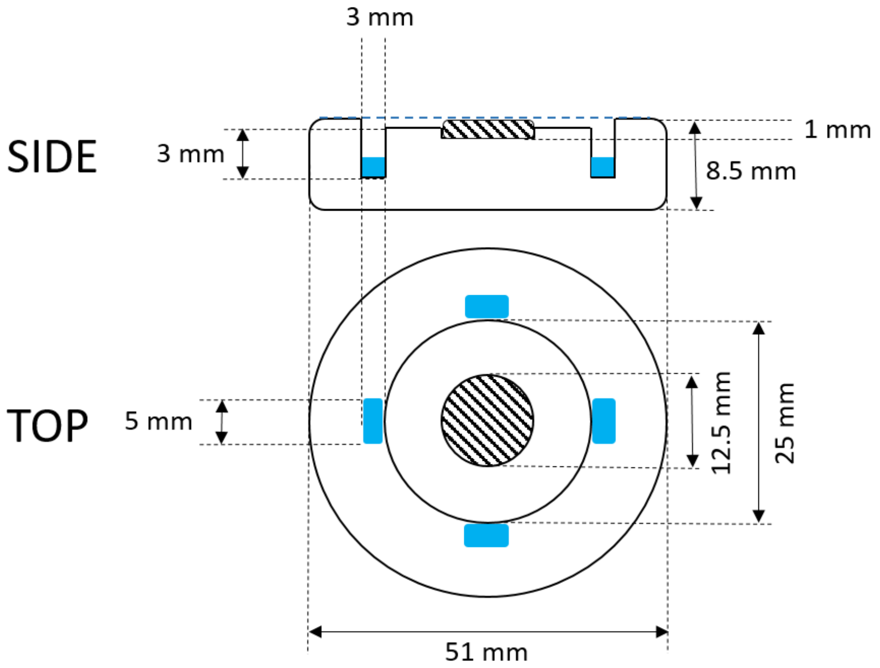

Figure S1. Design of the custom-made sample holder for *in situ* PXRD monitoring of samples under different vapour environments. The blue dashed line represents the PVC foil, and the striped square or circle represents the sample. The blue squares represent the liquid acting as a vapour source.

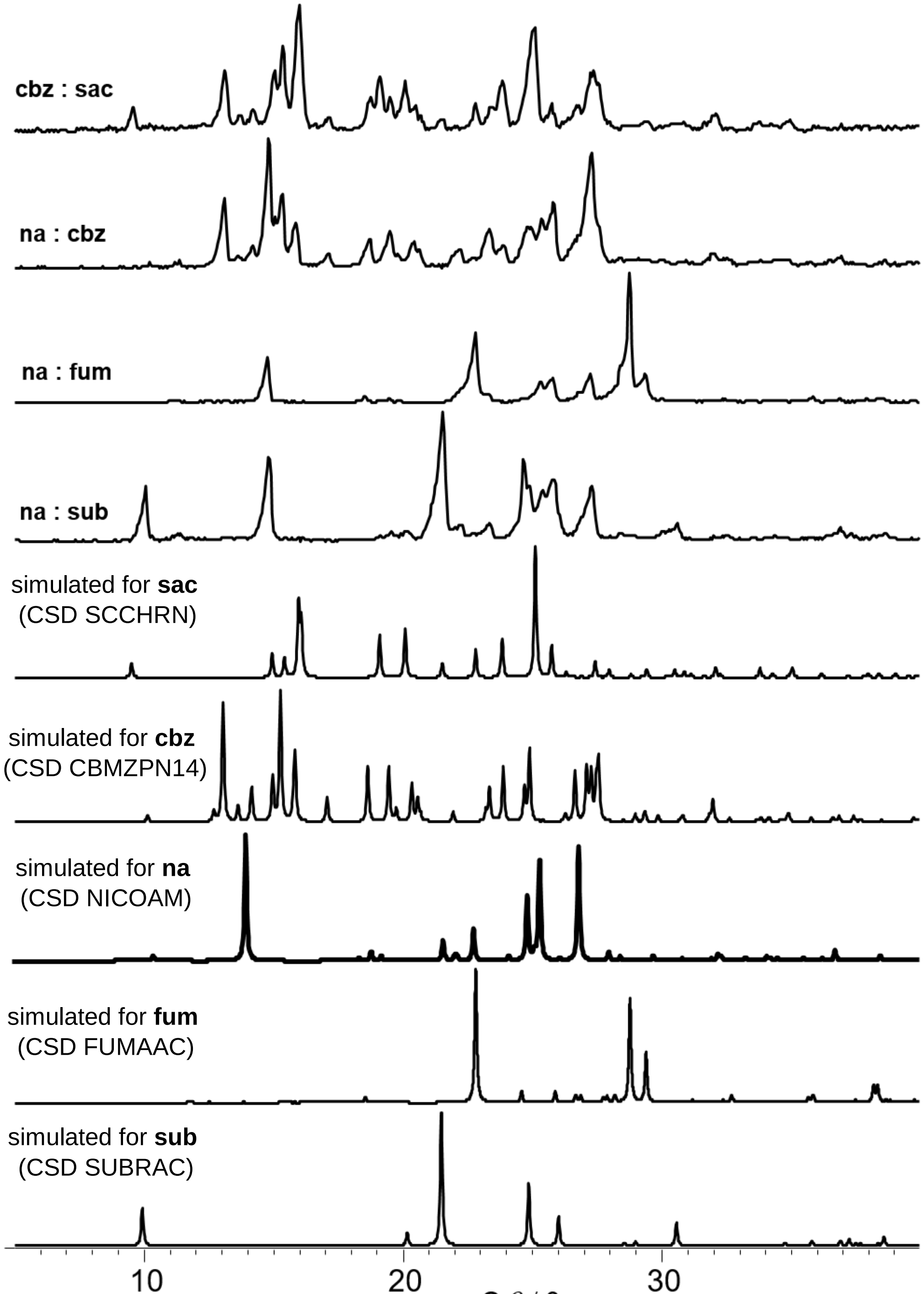

Figure S2. PXRD patterns for selected reaction mixtures immediately after mechanical mixing, compared to simulated diffractograms for saccharin (CSD SCCHRN) carbamazepine (CSD CBMZPN14), nicotinamide (CSD NICOAM), fumaric acid (CSD FUMAAC) and suberic acid (CSD SUBRAC), demonstrating the absence of any crystalline product.

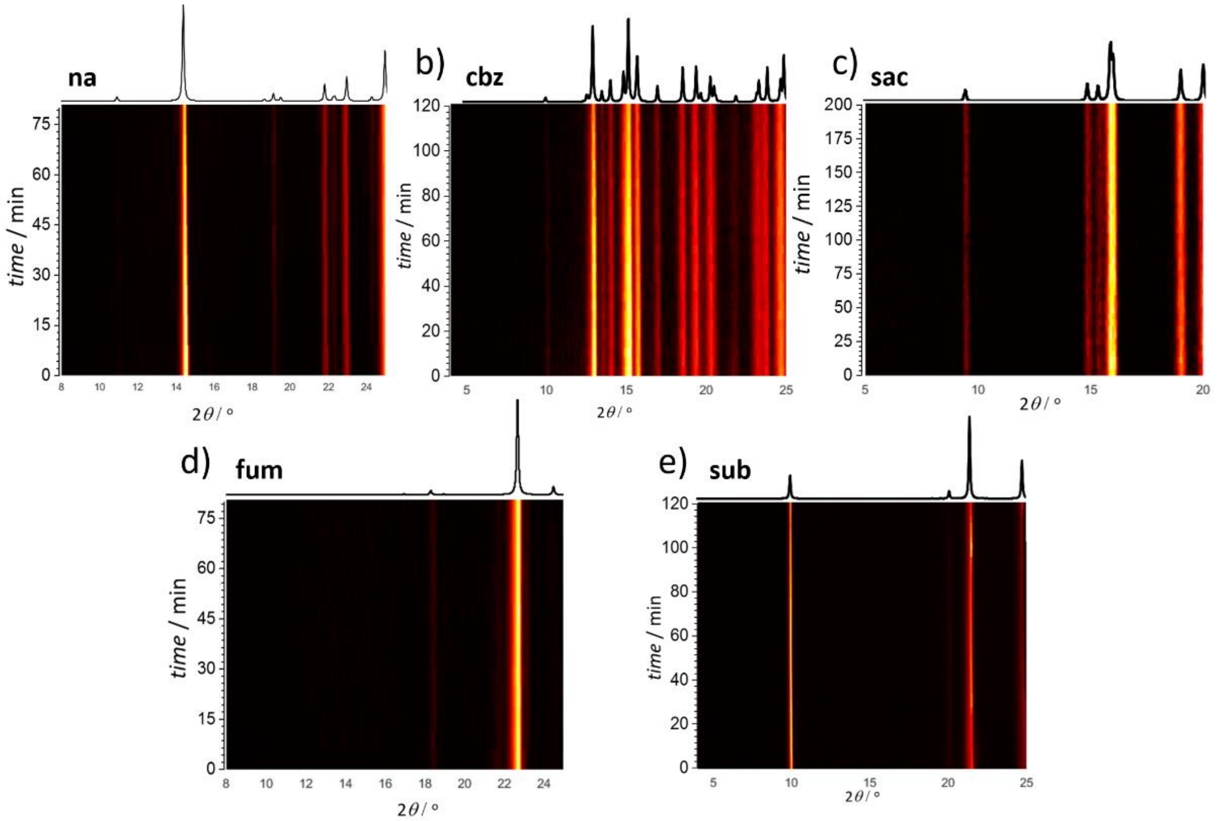

Figure S3. Time-resolved PXRD patterns for aging in MeOH vapours for all starting compounds used in this study. The PXRD patterns confirm the absence of polymorphic transformations or solvate formation.

2. Aging reaction of carbamazepine and nicotinamide

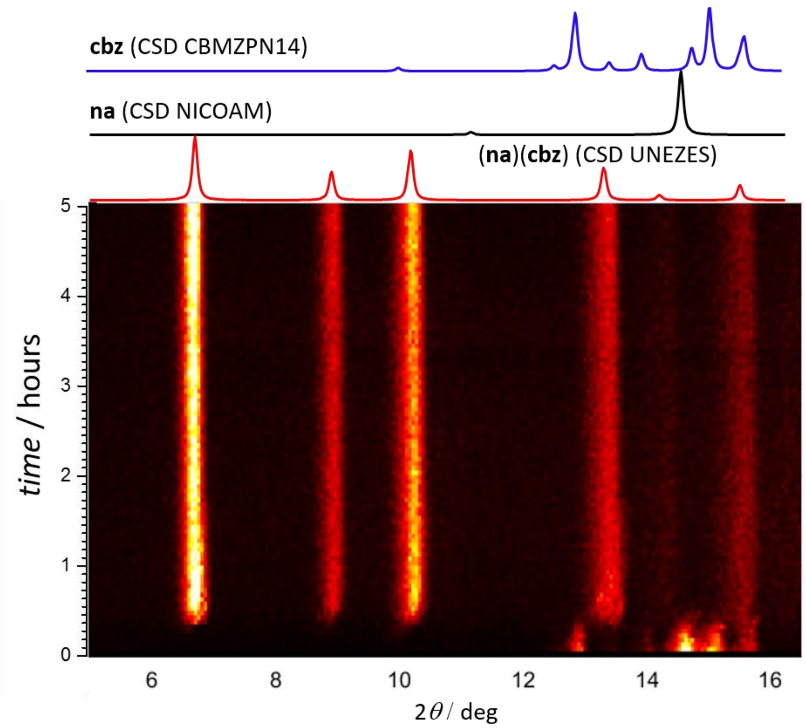

Figure S4. Time-resolved *in situ* collected X-ray powder diffractogram for the aging of a 1:1 stoichiometric mixture of **cbz** and **na** in MeOH, yielding the (**cbz**)(**na**) cocrystal. Time between individual scans is 2.83 minutes.

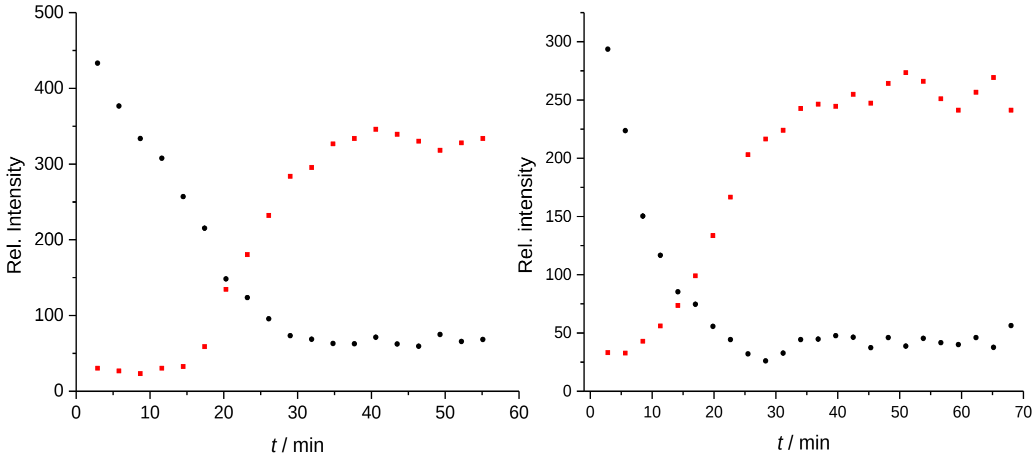

Figure S5. Time-dependent change in intensity of selected X-ray reflections for reactant **na** (●, (120), 2θ=14.45º) and product (**cbz**)(**na**) (■, (011), 2θ=6.50º) upon aging in: (left) MeOH vapour and (right) EtOH vapour. The profiles were obtained by averaging the intensity of individual reflections over a 2θ range of ± 0.1º.

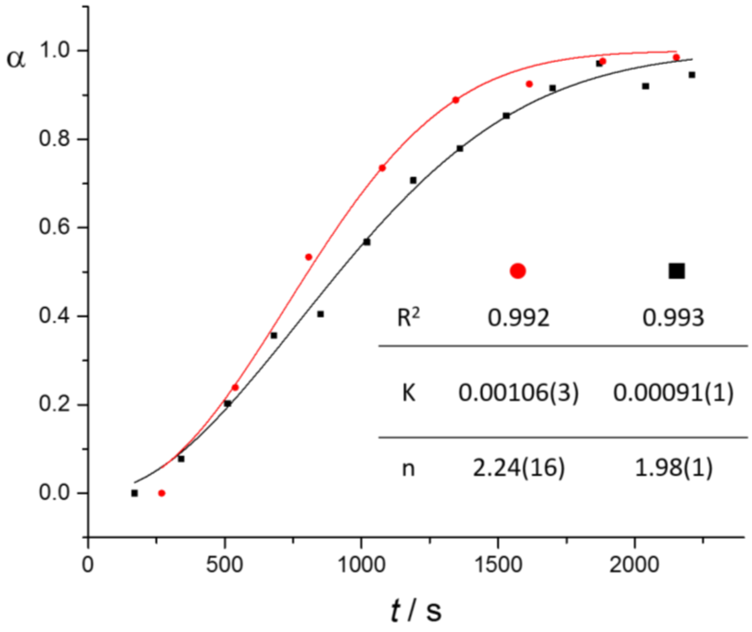

Figure S6. Fit of two sets of reaction profiles for the aging reaction of **na** and **cbz** in MeOH vapour to the JMAK model $\boldsymbol{\alpha} = \mathbf{1} - \boldsymbol{e}^{(-\boldsymbol{K}\boldsymbol{t})^{\boldsymbol{n}}}$. The α values correspond to normalised integrated intensities of the (011) X-ray reflection of (**cbz**)(**na**). Legend: ■, ● measured values, –, – calculated values. The data represent two sets of independent experiments.

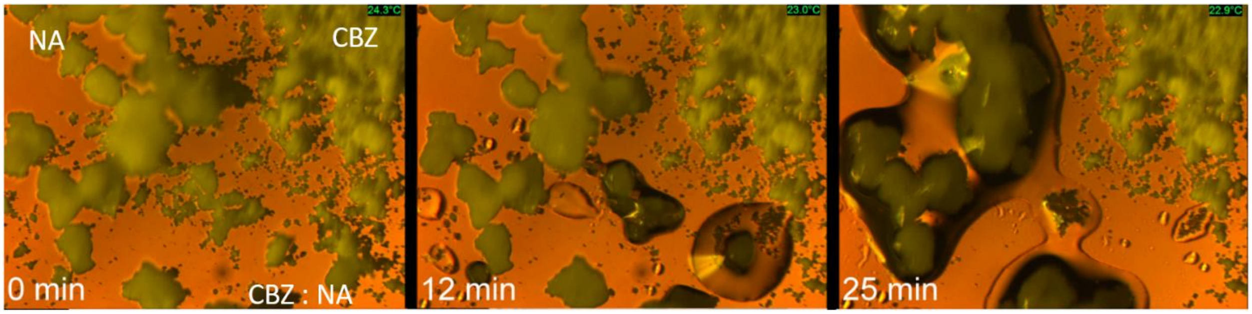

Figure S7. *In situ* microscopy of the reaction between **cbz** and **na** in MeOH vapours. Individual reactant powders were milled separately for 20 s and brought in contact under the microscope. Deliquescence occurs first on the solid mixture of reactants, where **cbz** and **na** solids are in direct contact, and then on the pure **na** sample. Pure **cbz** powder did not deliquesce during the experiment.

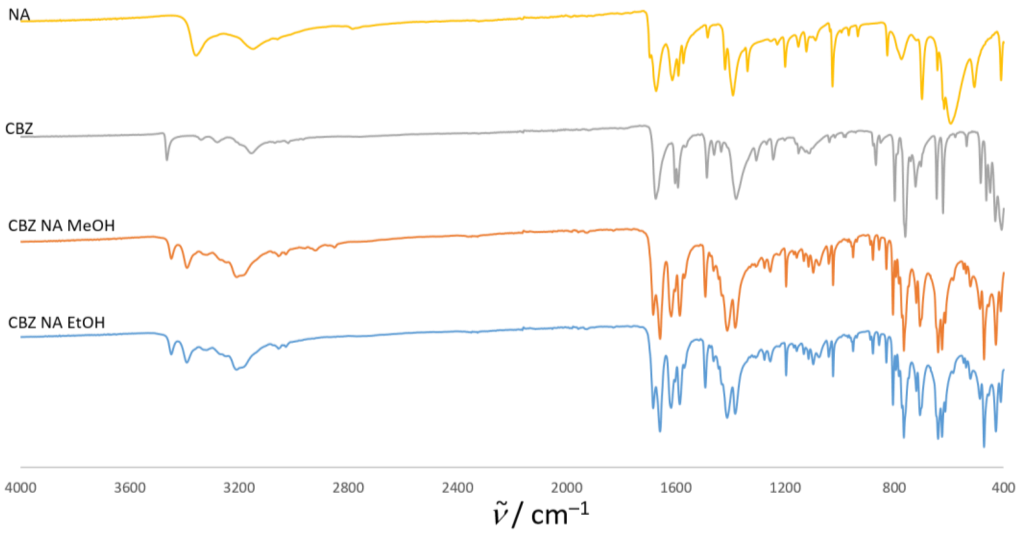

Figure S8. Comparison of FTIR-ATR spectra of (**cbz**)(**na**) obtained by aging in MeOH or EtOH vapour, along with spectra of starting compounds.

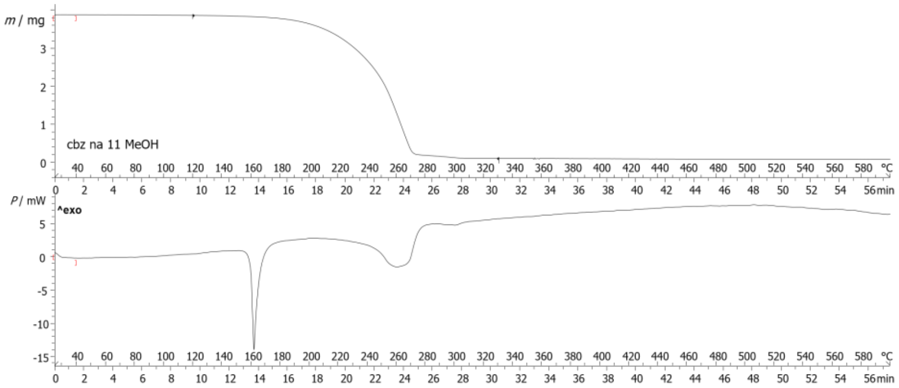

Figure S9. TGA/DSC thermograms of (**na**)(**cbz**) made by aging in MeOH vapour, heating rate 10 ºC/min in air (50 ml/min).

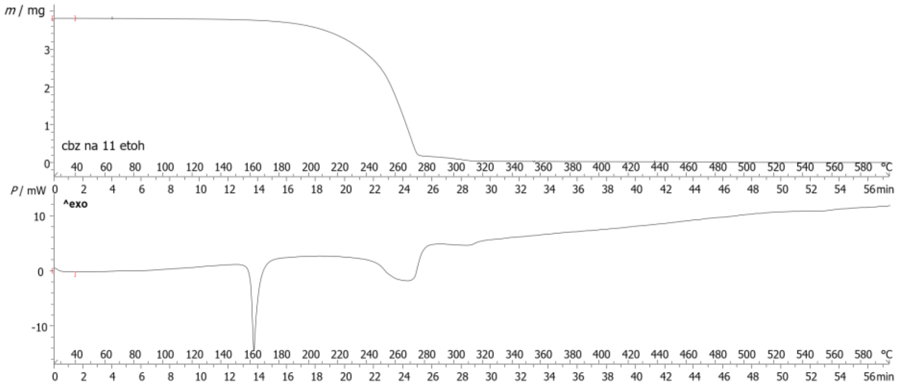

Figure S10. TGA/DSC thermograms of (**na**)(**cbz**) made by aging in EtOH vapour, heating rate 10 ºC/min in air (50 ml/min).

3. Aging reactions of carbamazepine and saccharin

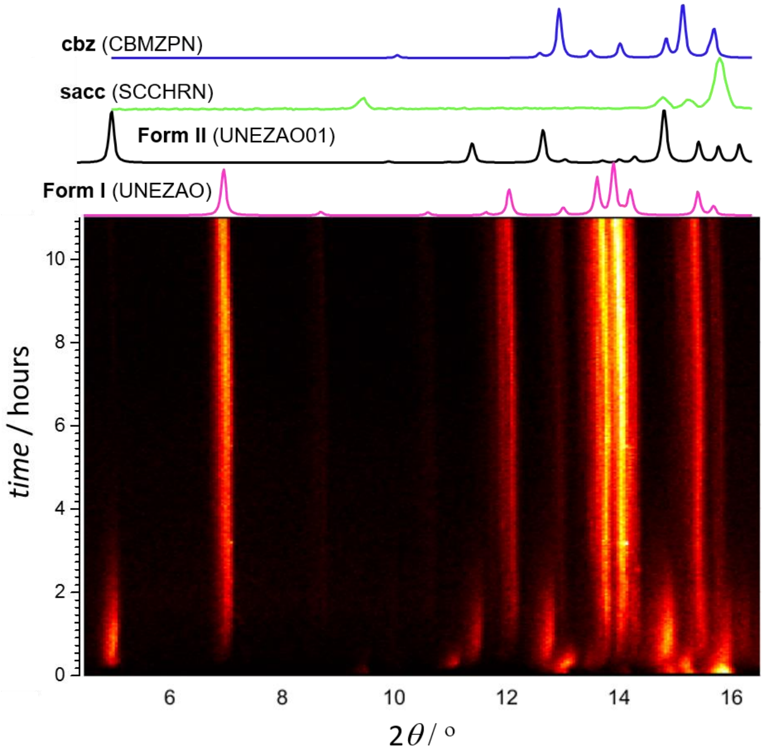

Figure S11. Time-resolved *in situ* collected X-ray powder diffractogram for the aging of the 1:1 stoichiometric mixture of **cbz** and **sac** in MeOH vapour. Time between individual scans is 2.75 minutes.

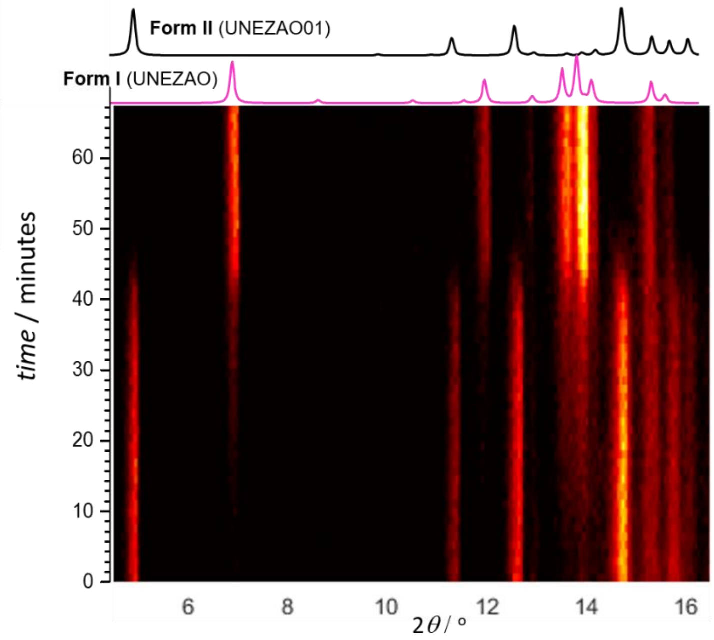

Figure S12. Time-resolved *in situ* collected X-ray powder diffractogram for the transformation of **(cbz)(sac)** Form II into Form I upon aging in MeOH vapour. Time between individual scans is 2.75 minutes.

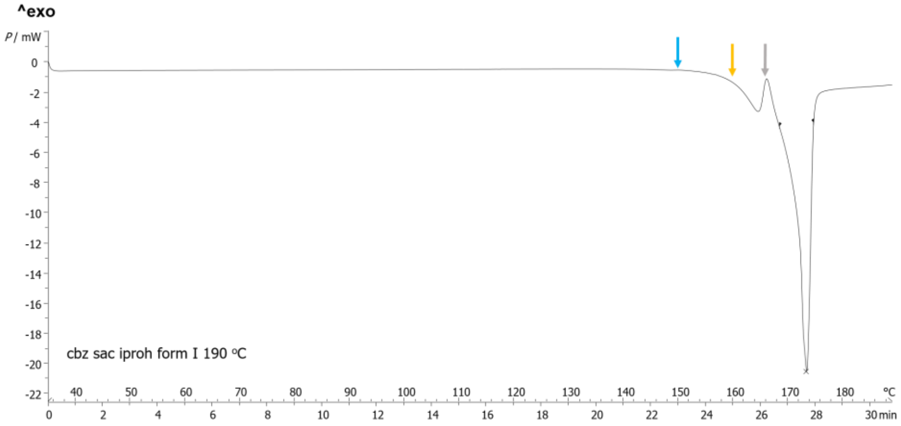

Figure S13. DSC thermogram of (**cbz**)(**sac**) Form II made by aging in *i*-PrOH vapour, heating rate 10 ºC/min in N_2 stream (50 ml/min. The measurement was repeated and stopped at different time intervals, denoted by differently coloured arrows (colour codes identical to those of FTIR-ATR spectra shown in Figure **S13** below), and the samples analysed by FTIR-ATR which revealed thermal interconversion of Form II into Form I.

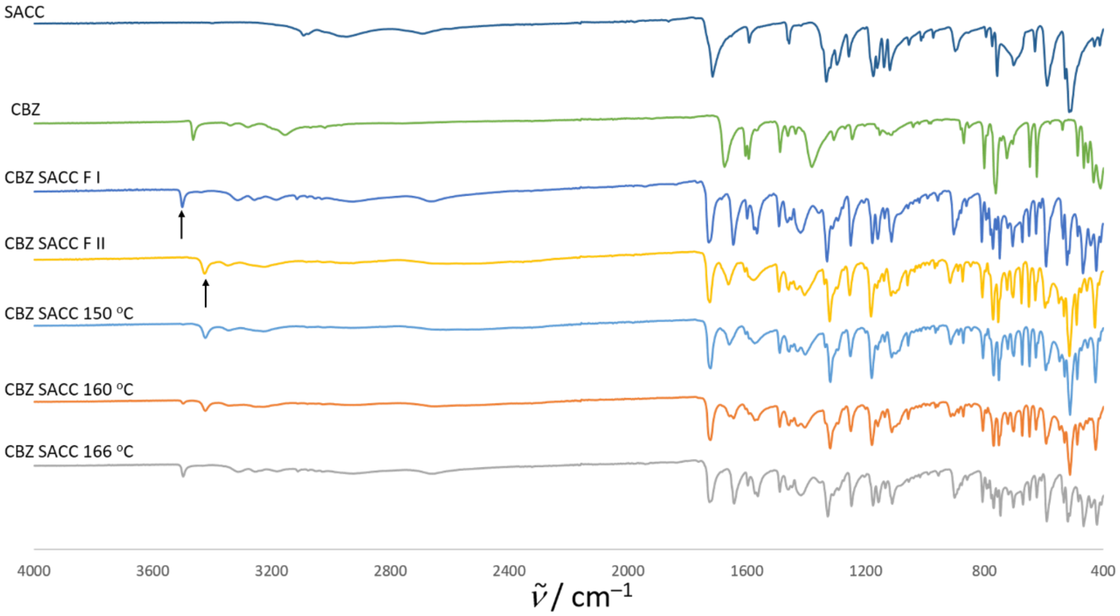

Figure S14. Comparison of FTIR-ATR spectra of (**cbz**)(**sac**) cocrystals after aging, along with spectra of the starting compounds. The "F I" and "F II" labels refer to Form I and Form II polymorphs of (**cbz**)(**sac**) (CSD codes UNEZAO and UNEZAO01, respectively). While the spectra of Form I and Form II of (**cbz**)(**sac**) are clearly distinguishable in the 1700-600 cm^{-1} region, the most pronounced differences are observed in N–H stretching region (*e.g.* bands at 3450 and 3380 cm^{-1}, denoted with arrows).

The spectra denoted with "150 ºC", "160 ºC" and "166 ºC" are for samples obtained by aging in *i*-PrOH (Form II), after heating to indicated temperature (see Figure **S12** for more details), demonstrating the thermal interconversion of Form II into Form I (**cbz**)(**sac**) above 160 ºC.

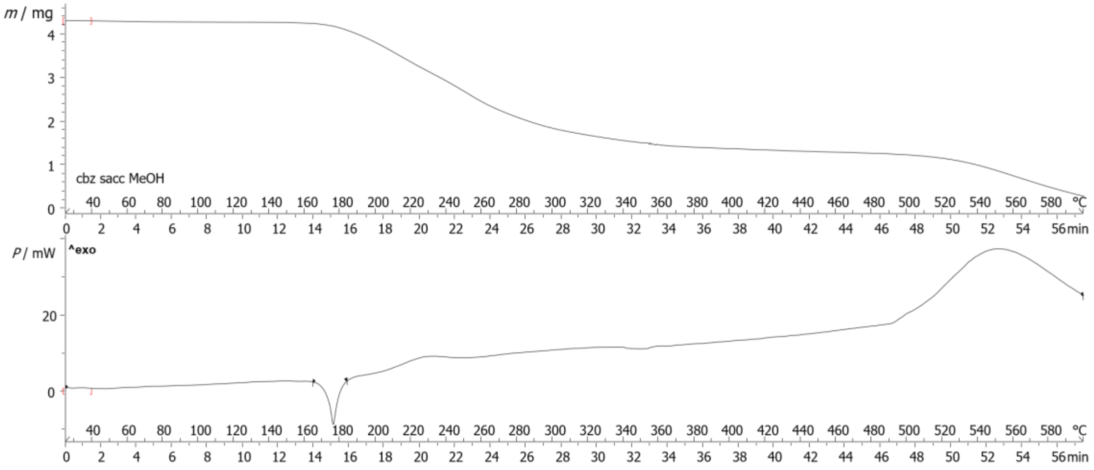

Figure S15. TGA/DSC thermogram of (**cbz**)(**sac**) made by aging in MeOH vapour, heating rate 10 °C/min in N_2 (50 ml/min).

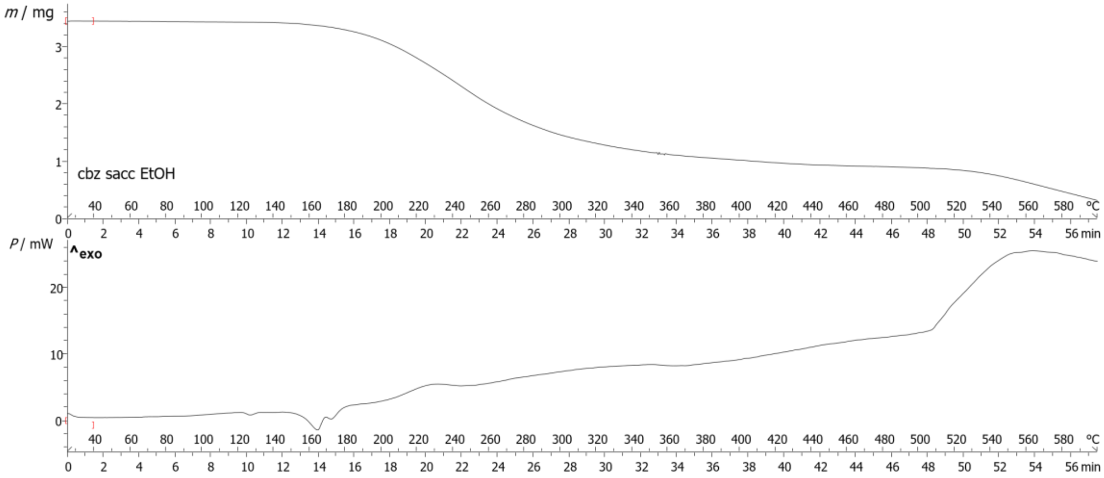

Figure S16. TGA/DSC thermogram of (**cbz**)(**sac**) made by aging in EtOH vapour, heating rate 10 °C/min in N_2 (50 ml/min)

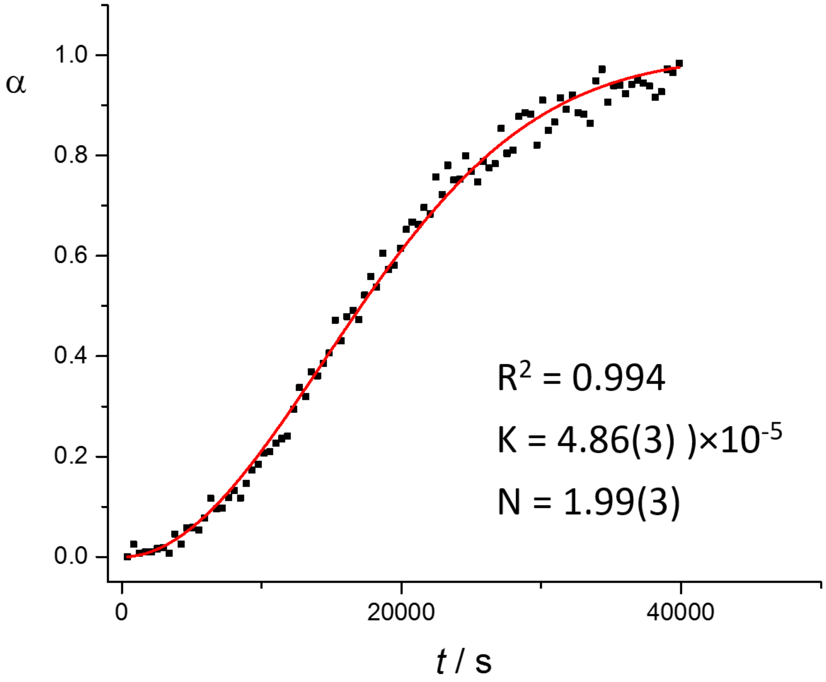

Figure S17. Fit of the reaction profile for the aging reaction of **cbz** and **sac** in *i*-PrOH vapour to the JMAK model $\boldsymbol{\alpha = 1 - e^{(-Kt)^n}}$. The α values correspond to normalised integrated intensity of the selected (200) X-ray reflection of Form II (**cbz**)(**sac**). Legend: ■ measured values, – calculated values.

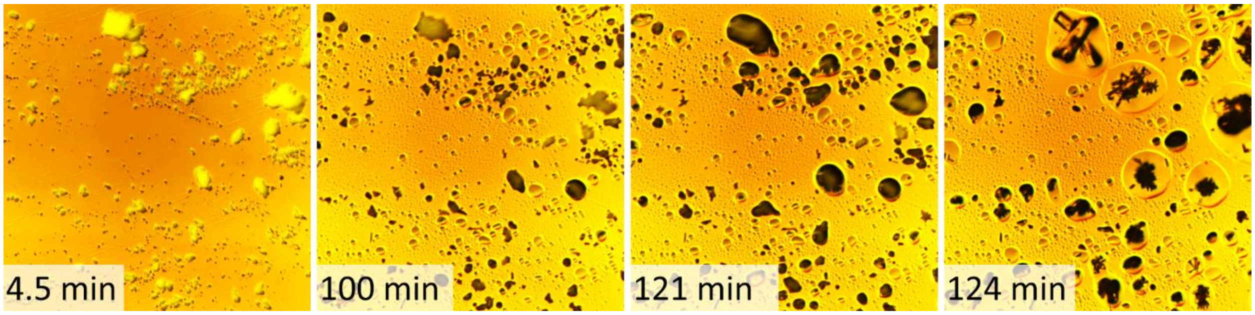

Figure S18. *In situ* microscopy of for the reaction of **cbz** and **sac** in MeOH vapour. The reactants powders were milled together for 20 s at 30 Hz and placed in contact under the microscope, in a closed vessel saturated with MeOH vapour.

4. Aging reactions of nicotinamide and suberic acid

4.1 Aging synthesis of the (na)(sub) cocrystal

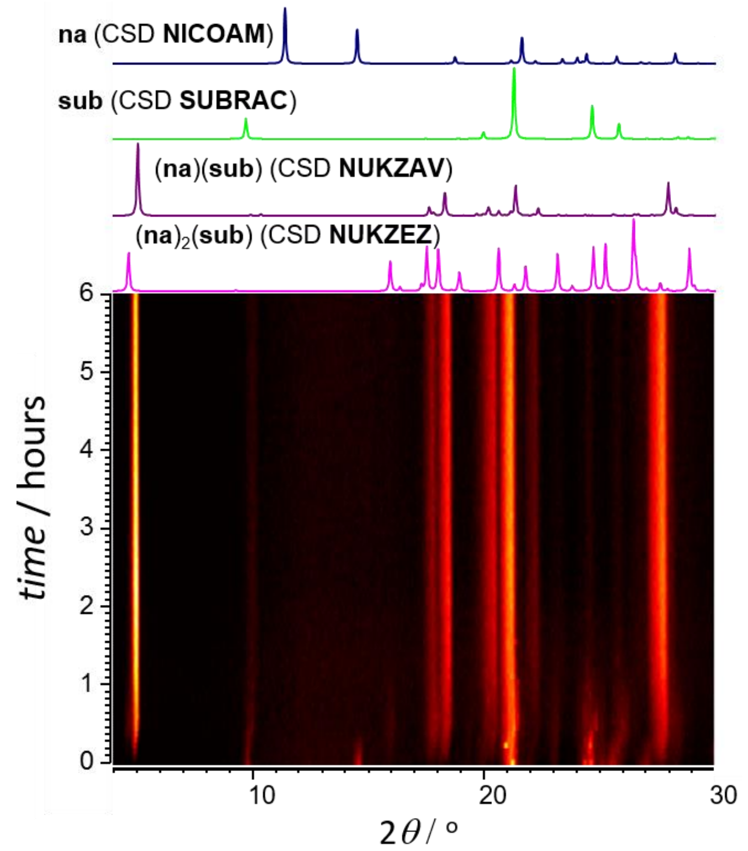

Figure S19. Time resolved *in situ* X-ray powder diffractogram for the aging of a 1:1 stoichiometric mixture of **na** and **sub** in MeOH vapour. The time between individual scans is 4.9 minutes.

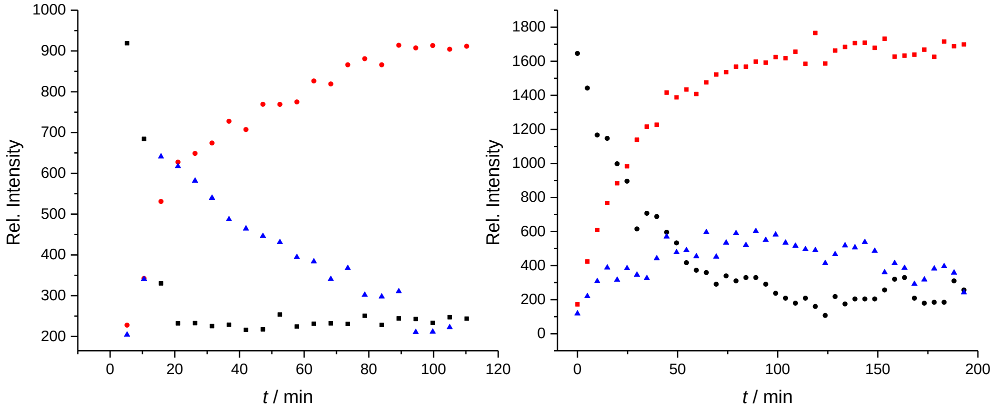

Figure S20. Time-dependent change in intensity of selected X-ray reflections for reactant **na** (■, (120), 2θ=14.45º) and products (**na**)(**sub**) (●, (020), 2θ=5.08º) and (**na**)$_2$(**sub**) (▲, (010), 2θ=16.20º) upon aging of a 1:1 stoichiometric mixture of **na** and **sub** in: (left) MeOH vapour and (right) EtOH vapour. The profiles were obtained by averaging the intensity of individual reflections over a 2θ range of ± 0.1º.

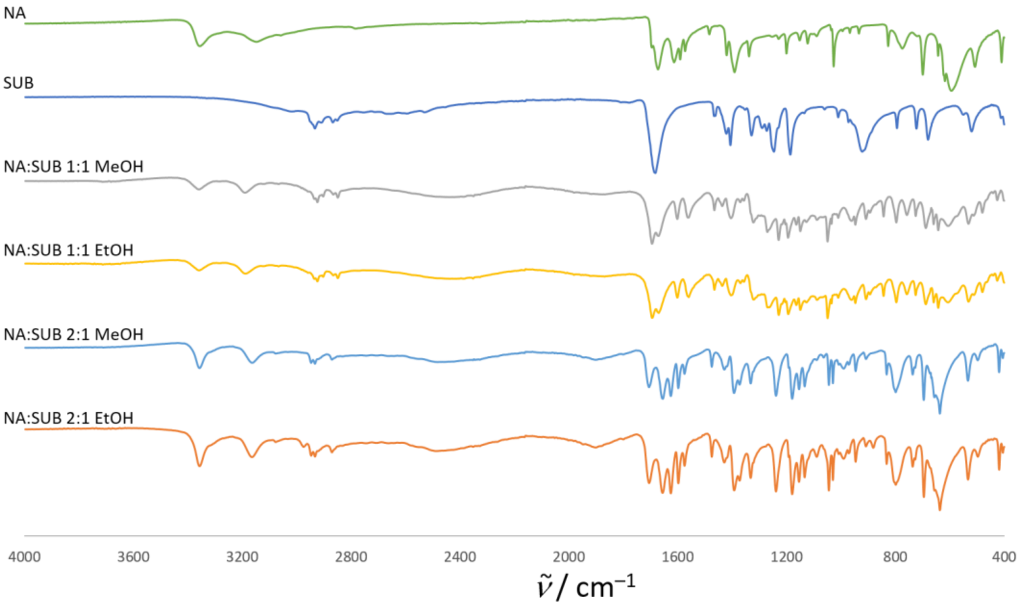

Figure S21. FTIR-ATR spectra of (**na**)(**sub**) after aging in MeOH and EtOH vapour. The spectra of starting compounds are provided for comparison**.**

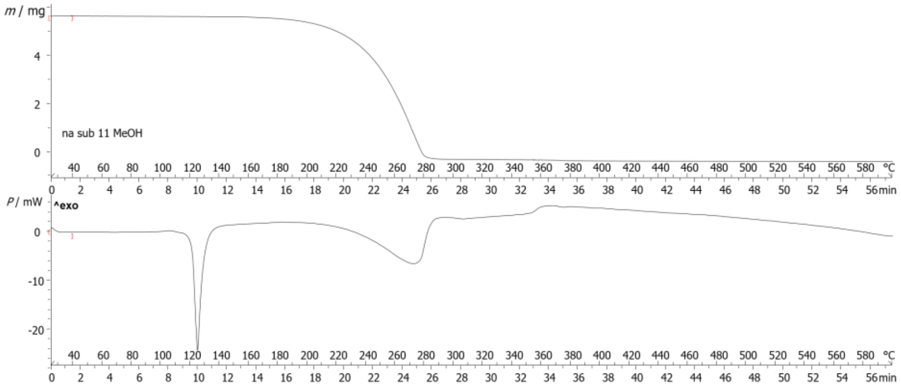

Figure S22. TGA/DTA curves of (**na**)(**sub**) cocrystal made by aging in MeOH vapour, heating rate 10 ^{o}C/min in air (50 ml/min).

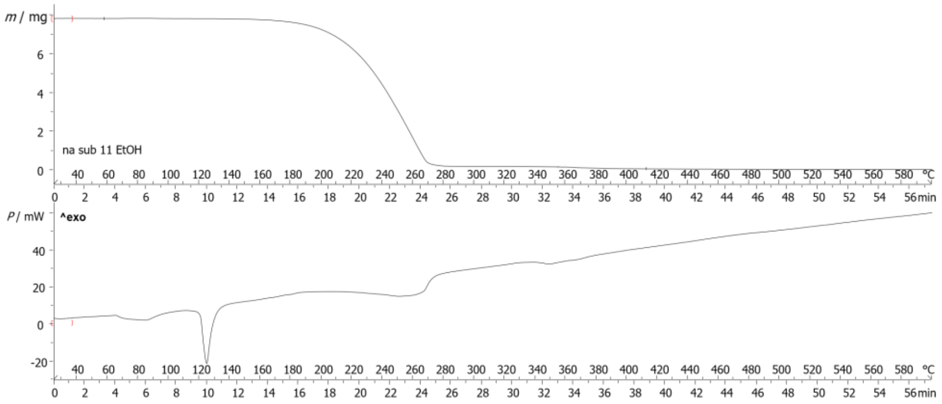

Figure S23. TGA/DSC curves of (**na**)(**sub**) cocrystal made by aging in EtOH vapour, heating rate 10 ^{o}C/min in air (50 ml/min).

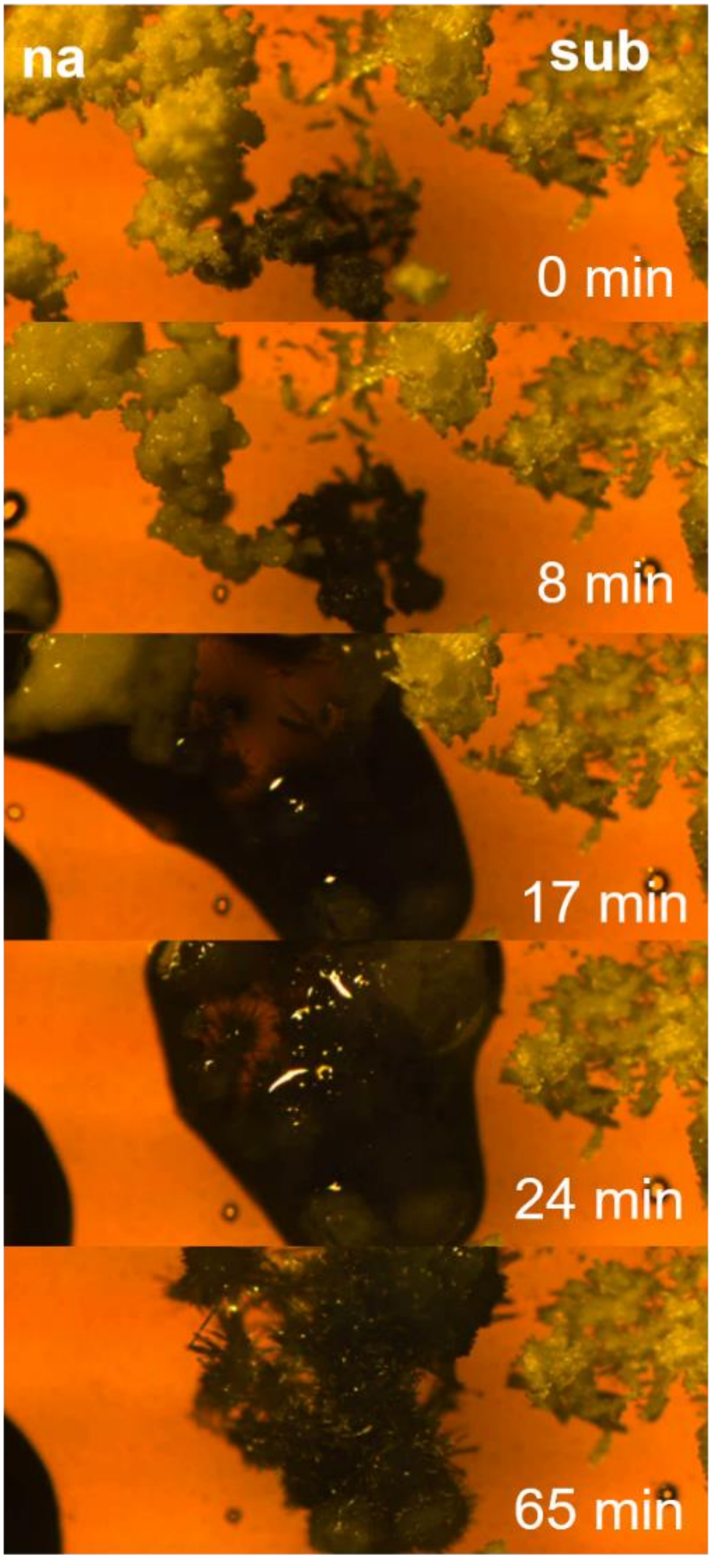

Figure S24. *In situ* microscopy of for aging reaction of **na** and **sub** in MeOH vapour. The individual reactants were milled separately for 20 seconds and brought in contact under the microscope. Deliquescence of the sample begins on **na**, envelops the sample of **sub**, and leads to formation of cocrystals and drying up of the sample.

4.2 Aging synthesis of the (na)$_2$(sub) cocrystal

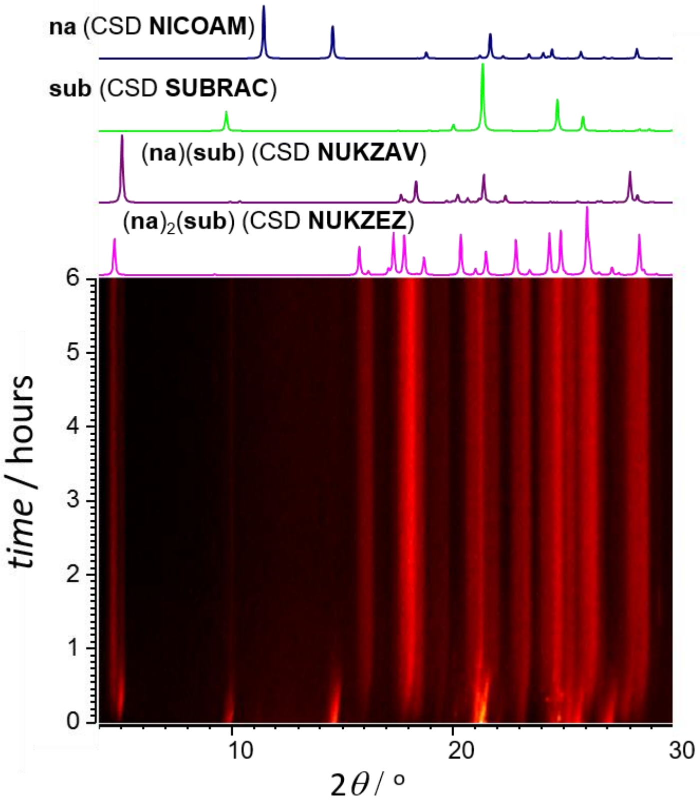

Figure S25. Time resolved *in situ* X-ray powder diffractogram for the aging reaction between **na** and **sub** (stoichiometric ratio *2*:1) in MeOH vapour. Time between individual scans is 4.9 minutes. The rightwards shift in the position of the peaks is an artefact of change in sample height due to change in its volume.

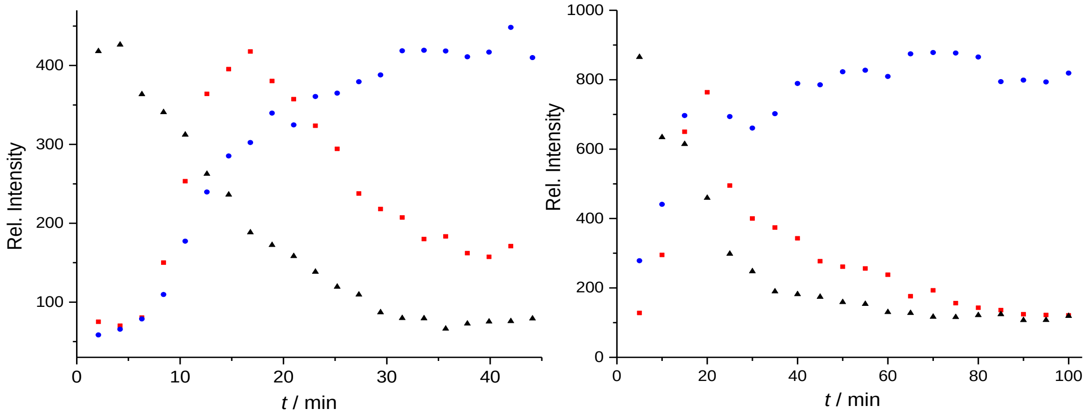

Figure S26. Time-dependent change in intensity of selected X-ray reflections for reactant **na** (■, (120), 2θ=14.45º) and products (**na**)(**sub**) (●, (020), 2θ=5.08º) and (**na**)$_2$(**sub**) (▲, (010), 2θ=16.20º) upon aging of a 2:1 stoichiometric mixture of **na** and **sub** in: (left) MeOH vapour and (right) EtOH vapour. The profiles were obtained by averaging the intensity of individual reflections over a 2θ range of ± 0.1º.

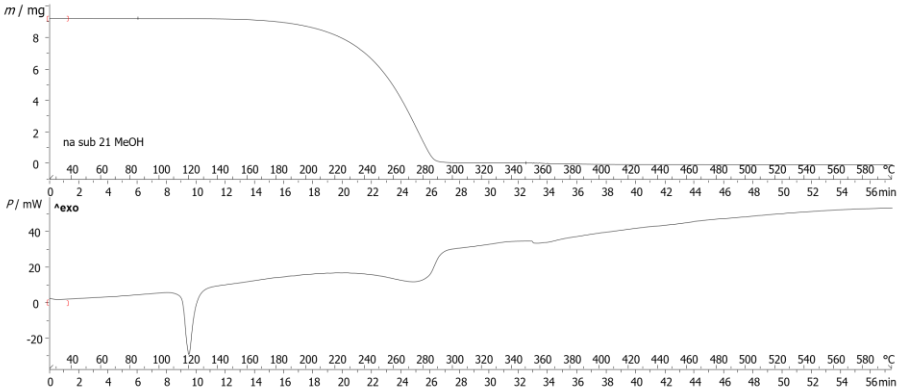

Figure S27. TGA/DSC thermograms of (**na**)$_2$(**sub**) made by aging in MeOH, heating rate 10 ^{o}C/min in air (50 ml/min).

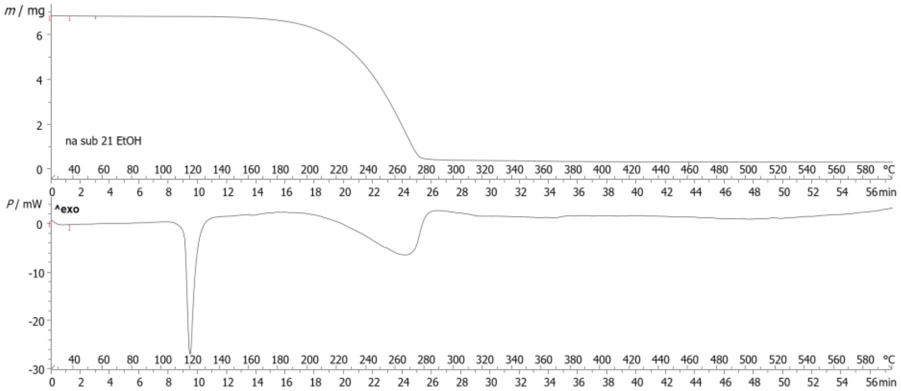

Figure S28. TGA/DSC thermograms of (**na**)$_2$(**sub**) made by aging in EtOH, heating rate 10 ^{o}C/min in air (50 ml/min).

5. Aging syntheses of cocrystals of nicotinamide and fumaric acid

5.1Aging synthesis of the (na)(fum) cocrystal

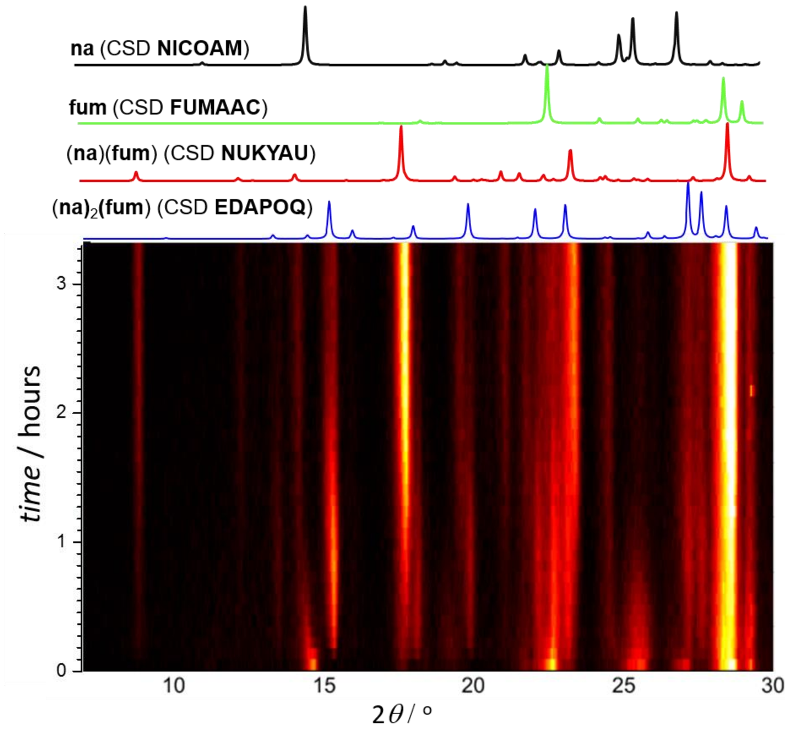

Figure S29. Time-resolved *in situ* collected X-ray powder diffractogram for the aging of a 1:1 stoichiometric mixture of **na** and **fum** in MeOH vapour. The time between individual scans is 4.9 minutes.

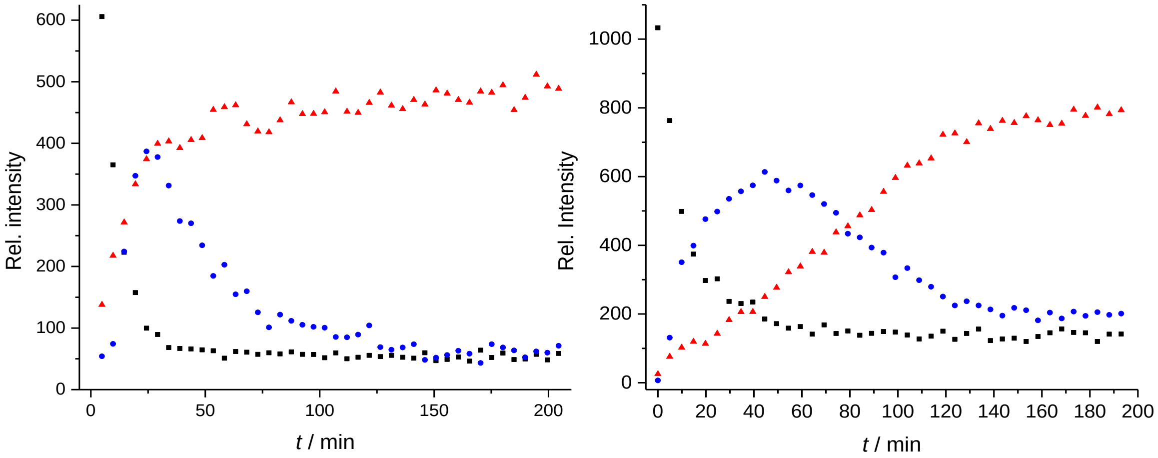

Figure S30. Time-dependent change in intensity of selected X-ray reflections for reactants **na** (■, (120), 2θ=14.45°) and products (**na**)(**fum**) (▲, (022), 2θ=17.90°) and (**na**)$_2$(**fum**) (●, (012), 2θ=15.40°) upon aging of a 1:1 stoichiometric mixture of **na** and **fum** in: (left) MeOH vapour and (right) EtOH vapour. The profiles were obtained by averaging the intensity of individual reflections over a 2θ range of ± 0.1°.

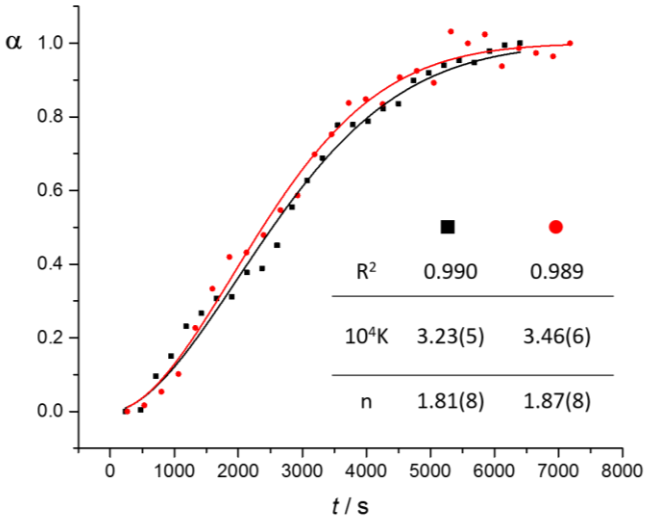

	■	●
R^2	0.990	0.989
10^4K	3.23(5)	3.46(6)
n	1.81(8)	1.87(8)

Figure S31. Fit of two sets of reaction profiles for the aging reaction of **na** and **fum** in MeOH vapour to the JMAK model $\boldsymbol{\alpha} = \mathbf{1} - \boldsymbol{e}^{(-\boldsymbol{K}\boldsymbol{t})^{\boldsymbol{n}}}$. The α values correspond to normalised integrated intensities of the characteristic (022) X-ray reflection of (**na**)(**fum**). Legend: ■, ● measured values, –, – calculated values. The data represents two sets of independent experiments.

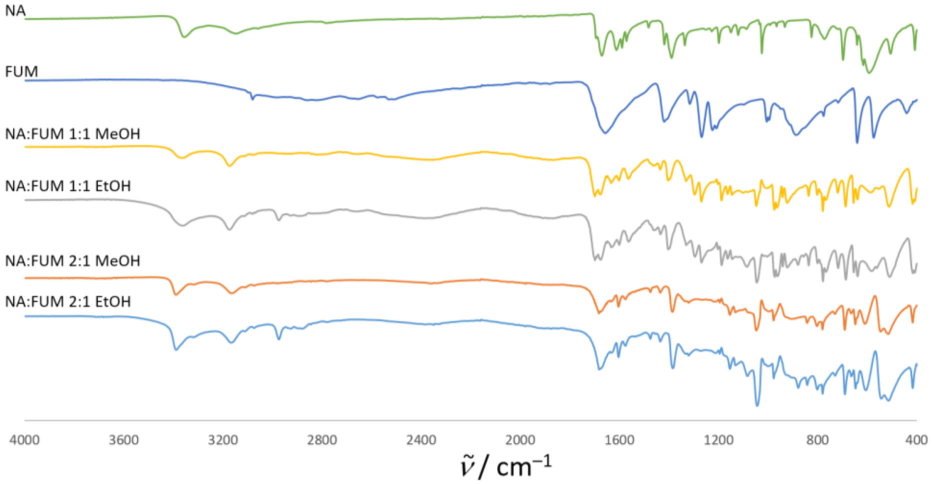

Figure S32. FTIR-ATR spectra of (**na**)(**fum**) after aging in MeOH and EtOH vapours, with spectra of reactants also shown**.**

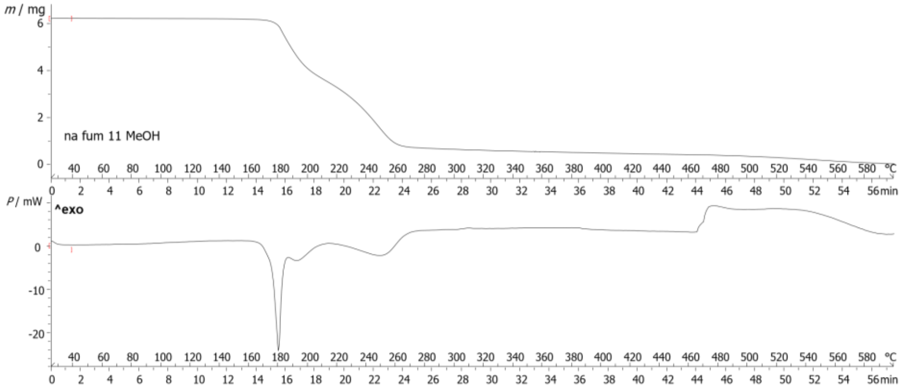

Figure S33. TGA/DTA thermograms of (**na**)(**fum**) made by aging in MeOH vapour, heating rate 10 °C/min in an air stream of 50 ml/min.

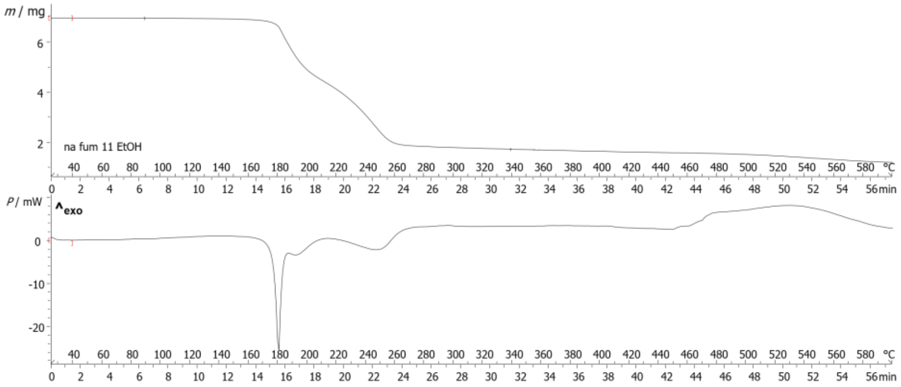

Figure S34. TGA/DSC thermograms of (**na**)(**fum**) made by aging in EtOH vapour, heating rate 10 ºC/min in air stream (50 ml/min).

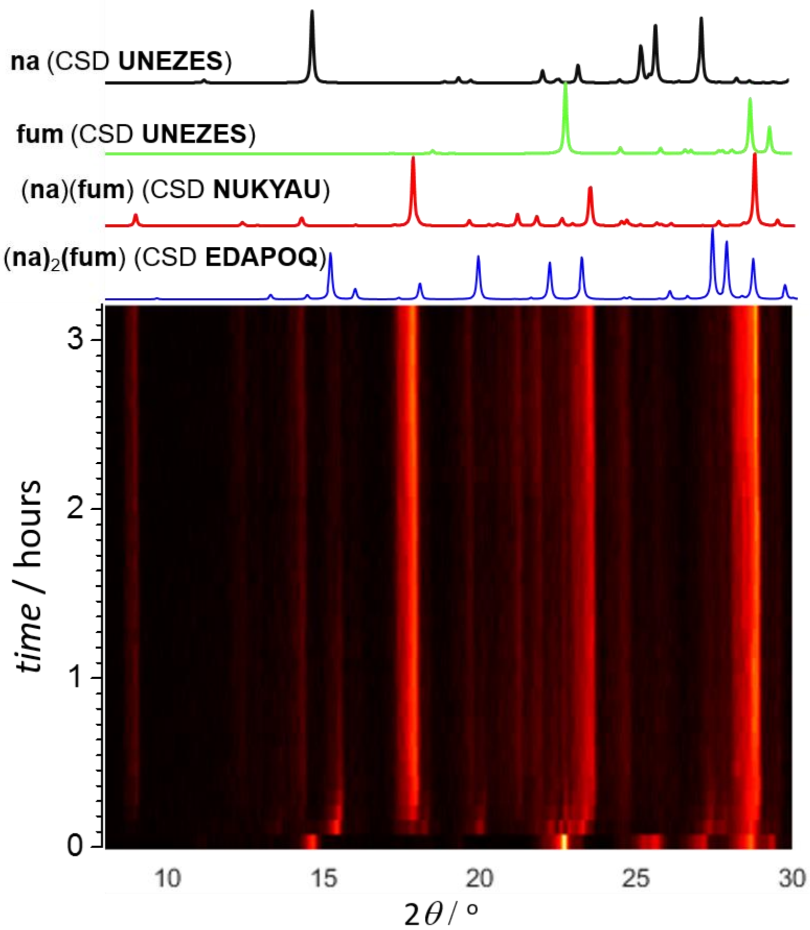

Figure S35. Time-resolved *in situ* obtained X-ray powder diffractogram for another aging reaction of a 1:1 stoichiometric mixture of **na** and **fum** in MeOH vapour. Time between individual scans is 4.9 minutes, and the emergence of (**na**)$_2$(**fum**) is best seen by a diffraction line at $2\theta \approx 15.2$, demonstrating reproducibility (see Figure **S28**).

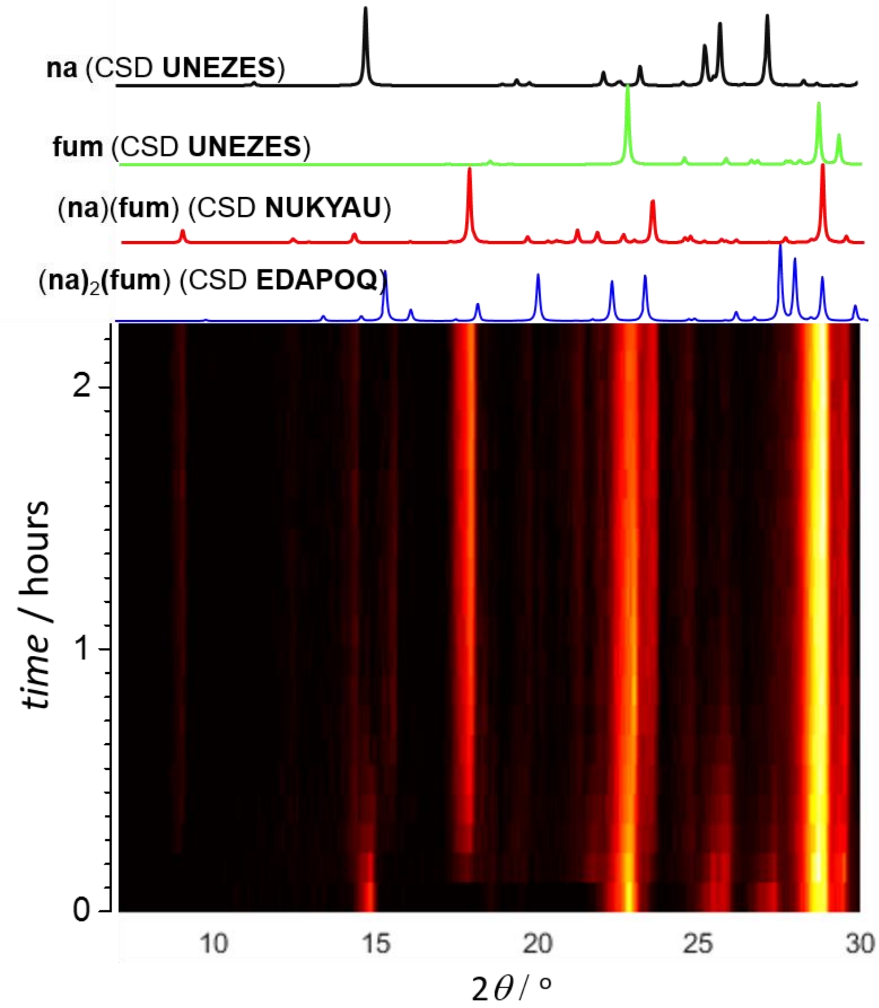

Figure S36. Time-resolved *in situ* X-ray powder diffractogram for the aging of a 1:2 stoichiometric mixture of **na** and **fum** in MeOH vapour. Time between individual scans is 4.9 minutes, and emergence of (**na**)$_2$(**fum**) is best seen by an X-ray diffraction line at $2\theta \approx 15.2^{\circ}$.

5.2Aging synthesis of the (na)$_2$(fum) cocrystal

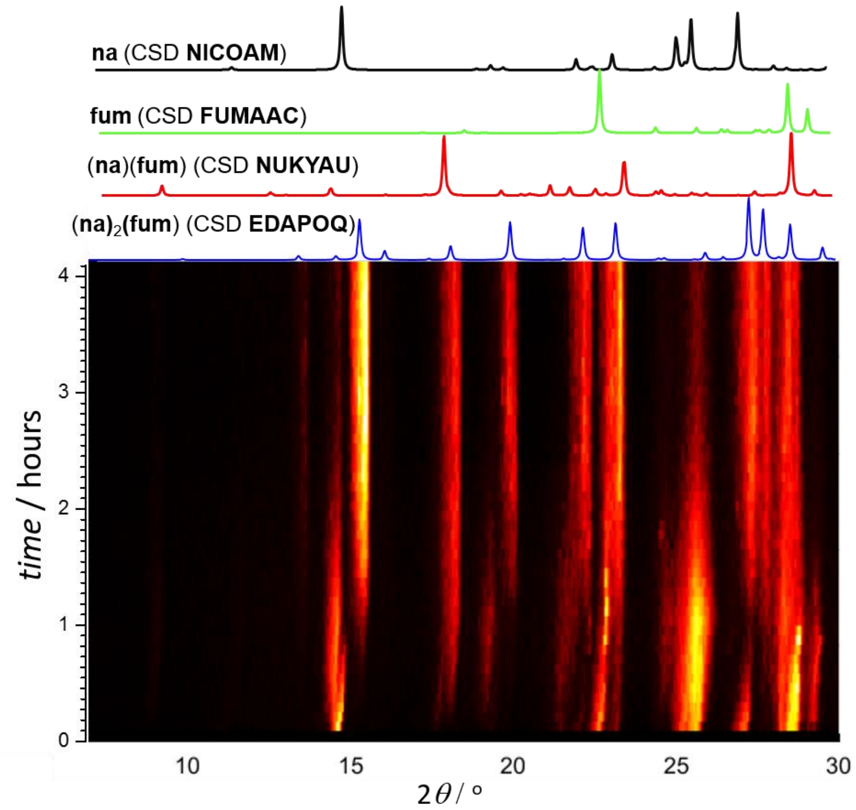

Figure S37. Time-resolved *in situ* X-ray powder diffractogram for the aging of a 2:1 stoichiometric mixture of **na** and **fum** in MeOH vapour. The time between individual scans is 4.9 minutes.

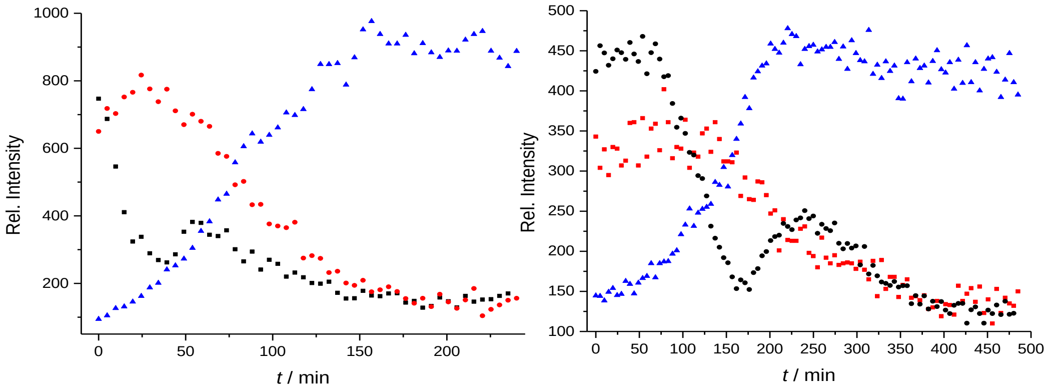

Figure S38. Time-dependent change in intensity of selected X-ray reflections for reactant **na** (●, (120), 2θ=14.45º) and products (**na**)(**fum**) (■, (021), 2θ=14.82º) and (na)$_2$(fum) (▲, (012), 2θ=15.40º) upon aging of a 2:1 stoichiometric mixture of **na** and **fum** in: (left) MeOH vapour and (right) EtOH vapour. The profiles were obtained by averaging the intensity of individual reflections over a 2θ range of ± 0.05º. The increase in intensity for (120) reflection of **na** around 50 min is an artefact of change in sample height during reaction and overlap with neighboring reflection.

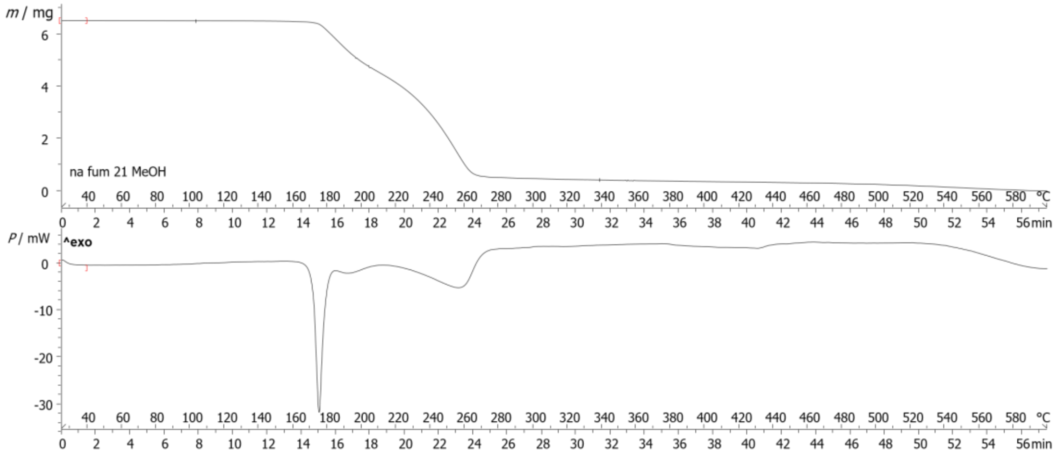

Figure S39. TGA/DSC thermogram of (**na**)$_2$(**fum**) made by aging in MeOH vapour, heating rate 10 °C/min in air (50 ml/min).

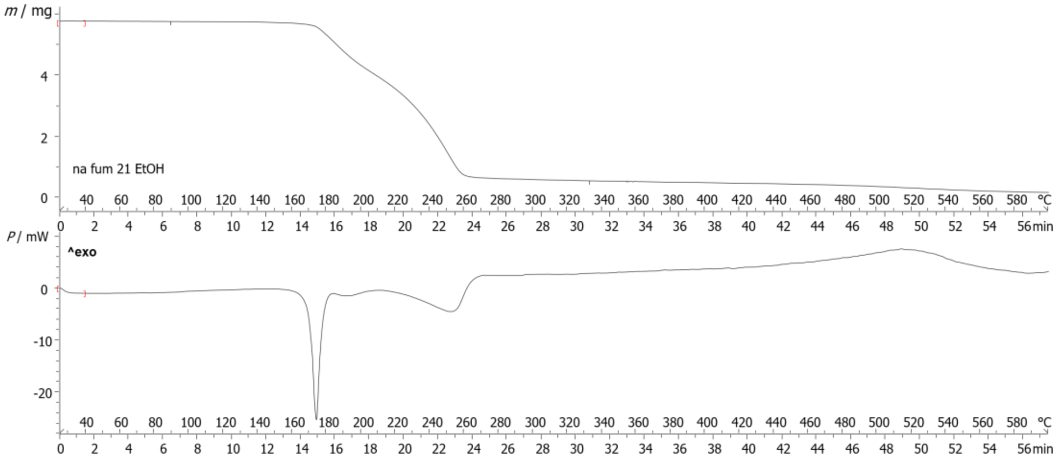

Figure S40. TGA/DSC thermograms of (**na**)$_2$(**fum**) made by aging in EtOH, heating rate 10 °C/min in air (50 ml/min).